Environ Sci Pollut Res (2013) 20:1511–1525
DOI 10.1007/s11356-012-0973-2

RESEARCH ARTICLE

Removal of heavy metal ions from wastewater by a novel HEA/AMPS copolymer hydrogel: preparation, characterization, and mechanism

Zhengkui Li · Yueming Wang · Ningmei Wu · Qichun Chen · Kai Wu

Received: 12 April 2012 / Accepted: 7 May 2012 / Published online: 22 May 2012

Abstract This study aims to synthesize 2-hydroxyethyl acrylate (HEA) and 2-acrylamido-2-methylpropane sulfonic (AMPS) acid-based hydrogels by gamma radiation and to investigate their swelling behavior and heavy metal ion adsorption capabilities. The copolymer hydrogels prepared were characterized via scanning electron microscopy, Fourier transformed infrared spectra, thermal gravimetric analysis, and X-ray photoelectron spectroscopy. The research showed that the copolymer hydrogel was beneficial for permeation due to its porous structure. In addition, the experimental group A-2-d [70 % water volume ratio and (*n* (AMPS)/*n* (HEA))=1:1] was an optimal adsorbent. The optimal pH was 6.0 and the optimal temperature was 15 °C. Pb^{2+}, Cd^{2+}, Cu^{2+}, and Fe^{3}+ achieved adsorption equilibriums within 24 h, whereas Cr^{3+} reached equilibrium in 5 h. Pb^{2}+, Cd^{2+}, Cr^{3+}, and Fe^{3+} maximum load capacity was 1,000 mg L^{-1}, whereas the Cu^{2+} maximum capacity was 500 mg L^{-1}. The priority order in the multicomponent adsorption was Cr^{3+}>Fe^{3+}>Cu^{2+}>Cd^{2+}>Pb^{2+}. The adsorption process of the HEA/AMPS copolymer hydrogel for the heavy metal ions was mainly due to chemisorption, and was only partly due to physisorption, according to the pseudo-second-order equation and Langmuir adsorption isotherm analyses. The HEA/AMPS copolymer hydrogel was confirmed to be an effective adsorbent for heavy metal ion adsorption.

Keywords 2-Hydroxyethyl acrylate (HEA) · 2-Acrylamido-2-methylpropane sulfonic (AMPS) acid · Heavy metal adsorption · Multicomponent adsorption · Porous structure

Responsible editor: Vinod Kumar Gupta

Z. Li · Y. Wang · N. Wu · Q. Chen · K. Wu
State Key Laboratory of Pollutant Control and Resource Reuse, Nanjing 210046, People's Republic of China

Z. Li (✉) · Y. Wang · N. Wu · Q. Chen · K. Wu
School of the Environment, Nanjing University, 163 Xianlin Avenue, Nanjing 210046, People's Republic of China
e-mail: zhkuili@nju.edu.cn

Introduction

Many industries discharge heavy metal ions, which are responsible for ecological problems in aquatic environments (Srivastava et al. 1997; Gupta et al. 1999, 2010; Gupta and Ali 2000; Aguado et al. 2009). Heavy metal ions can be absorbed and accumulated by living organisms because they are nonbiodegradable and highly soluble in the aquatic environments (Ju et al. 2009). Some heavy metal ions, including Pb^{2+}, Cd^{2+}, Cu^{2+}, Cr^{3+}, and Fe^{3+}, are significantly toxic to humans if they are introduced into the food chain and ingested beyond prescribed concentrations (Gupta et al. 2007a; Gupta and Rastogi 2008a, 2009; Mohan and Sreelakshmi 2008).

Research on the removal of heavy metal ions from wastewater has attracted significant attention. Effective removal methods have been developed, including electrodeposition, filtration, reverse osmosis, precipitation, ion exchange, solvent extraction, and adsorption (Gupta et al. 2001, 2003; Gupta and Ali 2004, 2006; Miretzky et al. 2006). Adsorption is the most promising among these technologies due to its high efficiency, ease of operation, and cost effectiveness (Gupta et al. 2009; Gupta and Suhas 2009; Yildi et al. 2010). In this respect, copolymer hydrogels have attracted attention as the selected adsorbent for removing heavy metal ions from wastewater due to their ability of incorporating different chelation groups into the polymeric networks (Ali 2010;

Zheng et al. 2011). Copolymer hydrogels, which can be prepared with different functional groups, such as hydroxyl, amine, carboxylic acid, and sulfonic acid groups, are three-dimensional networks of hydrophilic polymers cross-linked by chemical or physical interactions. Due to their significant swelling in water, copolymer hydrogels are able to expand in volume in response to changes in external parameters, such as pH, temperature, and ionic strength (Zhao et al. 2005). Copolymer hydrogels can control the diffusion process and bind chemical species through their polar functional groups. These functional groups existing in cross-linked polymeric materials can be manipulated easily for specific applications, such as functioning as complex agents for heavy metal ion removal from wastewater (Wang et al. 2010). Therefore, copolymer hydrogels can be considered novel, highly responsive, and high-capacity adsorbent materials for the removal of heavy metal ions from wastewater (Zheng and Wang 2010).

The practical application of copolymer hydrogels has some disadvantages, such as the poor mechanical strength pertaining to their fragility in water and poor metal binding capacity in variable external water conditions (Ngah et al. 2004; Gupta et al. 2006a, b, 2012; Gupta and Rastogi 2008b). Copolymer hydrogel mechanical strength is related to water content and can be improved by the addition of a hydrophobic component to the hydrogel structure (Gupta et al. 2006b, c; Osifo et al. 2008; Saleh and Gupta 2012). Moreover, the inclusion of a hydrophobic constituent reduces the diffusion rate; hence, the selectivity of the copolymer hydrogel can be made more controllable (Essawy and Ibrahim 2004).

The current research focused on the analysis and characterizations of a novel copolymer hydrogel. The hydrogel-based 2-hydroxyethyl acrylate (HEA) and 2-acrylamido-2-methylpropane sulfonic acid (AMPS) copolymer were obtained by radiation-induced copolymerization using mixtures with different molar ratios at various moisture contents. The characteristics of the copolymer hydrogel were studied via scanning electron microscopy (SEM), Fourier transform infrared spectra (FTIR), thermal gravimetric analysis (TGA), and X-ray photoelectron spectroscopy (XPS). The Freundlich and Langmuir adsorption isotherm equations, as well as the pseudo-first-order and pseudo-second-order equations, were utilized to verify the mechanism and kinetics of the adsorption process. In addition, the competitive adsorption was studied in a multi-component heavy metal ion experiment.

Methods and materials

Materials

The HEA ($C_7H_{13}NO_4S$) and AMPS ($C_5H_8O_{3)}$ were purchased from Sigma-Aldrich (Saint Louis, USA). The molecular weights of AMPS and HEA were 207.25 and 116.12 g mol^{-1}, respectively. Pb^{2+}, Cd^{2+}, Cu^{2+}, Cr^{3+}, and Fe^{3+} ions were provided by $Pb(NO_3)_2$, $Cd(NO_3)_2{\cdot}4H_2O$, $Cu(NO_3)_2{\cdot}3H_2O$, $Cr(NO_3)_3{\cdot}9H_2O$, and $FeCl_3$, respectively. They were analytically pure and purchased from SINOPHARM (Shanghai, China).

Up to 1,000 mg L^{-1} heavy metal ion stock solutions were prepared by dissolving appropriate amounts of heavy metal ions in deionized water. The working solutions containing different concentrations of heavy metal ions were prepared by stepwise dilution of the stock solutions. The pH values were adjusted by the addition of 0.1 and 1.0 mol L^{-1} NaOH or HCl solutions to reach the required values (Mettler Toledo FE20 pH meter). The other reagents used were analytical grade and prepared with deionized water.

Preparation of HEA/AMPS copolymer hydrogel

The HEA/AMPS copolymer hydrogels were prepared by radiation-induced copolymerization of mixtures with different molar ratios at various moisture contents. First, aqueous HEA and AMPS solutions were prepared in deionized water (weight percent) with various compositions. The hydrogel components in different experimental groups are shown in Table 1. Second, before the ^{60}Co gamma ray treatment, the solution was purged with nitrogen gas for 20 min to eliminate any dissolved oxygen. Third, the mixtures were transferred to silicone molds 10×40×5 mm in size. The mixtures in the molds were covered with a transparent 30 lumen thick Teflon film to prevent oxygen inhibition. Fourth, the mixtures were irradiated with the ^{60}Co gamma ray source at 10 kGy for 24 h. The ^{60}Co gamma ray source is installed at the Nanjing Radiation Center. Fifth, the obtained copolymer hydrogels were removed from the molds and cut into pieces with 5×5×5 mm dimension. Finally, all samples were washed in excess deionized water to remove the unreacted components, and then dried in a vacuum oven (HZF-280, Shanghai Hong Yue Test Equipment Co., Ltd., China) at 28 °C for 72 h until constant weight was achieved.

Swelling

The prepared hydrogels were immersed in deionized water at 25 °C for 48 h at pH 7. After removal from water, the

Table 1 Components of hydrogels

Volume ratio of water (wt%)	AMPS (mol)/HEA (mol)			
	1:9	1:4	2:3	1:1
80	A-1-a	A-1-b	A-1-c	A-1-d
70	A-2-a	A-2-b	A-2-c	A-2-d
60	A-3-a	A-3-b	A-3-c	A-3-d

excess water on the hydrogel surfaces was discarded with absorbent paper. The AMPS content was described as n (AMPS)/(n (AMPS) + n (HEA)). The equilibrium degree of swelling (EDS) of the hydrogels was calculated as:

$$\mathrm{EDS} = \frac{W_S - W_O}{W_O} \quad (1)$$

where W_S and W_O are the weights of the swollen and the dry hydrogel, respectively.

Characterization of the copolymer hydrogel

The copolymer hydrogels were examined before and after treatments. The dried specimens were investigated for morphological details via SEM (S-3400 N II, Hitachi, Japan), and were coated with gold film using an acceleration voltage of 20 kV. XPS (PHI 5000 Versa Probe, Ulvac-Phi, Japan) was used to analyze the surface characteristics of the hydrogels. All the binding energies (BE) were referred to as 284.6 eV of the neutral C1 peak to compensate for the surface charging effect. The software XPS peak 4.1 was used to deconvolute the XPS spectra into the subcomponents at the surface. The FTIR of the hydrogel was recorded before and after the adsorption experiments via a NEXUS 870 Fourier transformation spectrometer (Nicolet, USA) with the range of 400–4,000 cm^{-1} by grinding the dried hydrogel with KBr. TGA was performed using the Perkin Elmer (USA) TGA system of Type Pyris 1 under a nitrogen atmosphere (20 mL min^{-1}). The temperature range was ambient (20–700 °C at a heating rate of 20 °C min^{-1}).

Heavy metal ion adsorptivity of the copolymer hydrogel

The adsorption properties of the hydrogels for heavy metal ions were investigated in batch experiments. In each experiment, the amount of dried hydrogel sorbent was kept at 0.1 g for a 50 mL solution in a 300 mL flask. The flasks were stirred magnetically at 200 rpm, and the pH was adjusted with 1 M HNO_3. After equilibrium was attained, the aqueous phases were separated from the hydrogels. Furthermore, a Z-8100 (Hitachi, Japan) Atomic Absorption Instrument was used for the determination of heavy metal ion concentrations in the solutions before and after treatments. The instrument responses were periodically calibrated with 1,000 ppm metal standard solutions (Merck, Germany). Every value reported in this research was an average of at least three separate measurements.

Single-component heavy metal ion adsorption

The effect of the compositions of the HEA/AMPS copolymer hydrogel on the single-component heavy metal ion adsorptivity was investigated initially. Then, the optimum values of the operating conditions (pH, temperature, and initial heavy metal ion concentration) and the characteristics of adsorption kinetics were studied with the hydrogel components in the experimental group A-2-c for convenience (Table 1).

The dry copolymer hydrogel samples of different compositions (Table 1) were equilibrated for 24 h in 1,000 mg L^{-1} single-component ion (Pb^{2+}, Cd^{2+}, Cr^{3+}, Cu^{2+}, and Fe^{3+}) solution at ambient temperature and pH 6 to investigate the effect of the composition of the HEA/AMPS copolymer hydrogels on single-component heavy metal ion adsorption. The dry copolymer hydrogel was immersed in a series of 1,000 mg L^{-1} single heavy metal ion solutions at pH 1, 2, 3, 4, 5, and 6 at room temperature for 24 h to study the optimum pH for maximum adsorption. The dry copolymer hydrogel samples were immersed in 1,000 mg L^{-1} single heavy metal ion solutions at pH 6 to examine the effect of temperature on heavy metal ion adsorption. The temperatures of the solutions were adjusted to 15, 20, 25, 30, 35, and 40 °C for 24 h.

The dry hydrogels were equilibrated at room temperature for 24 h in 1, 10, 50, 100, 200, 500, 1,000, and 2,000 mg L^{-1} single heavy metal ion solutions to study the effect of the initial heavy metal ion concentration on the adsorption capacity of hydrogel and adsorption isotherm. Pb^{2+}, Cd^{2+}, Cu^{2+}, and Cr^{3+} solutions were prepared in AcOH–NaAc buffer at pH 6, and that for Fe^{3+} was prepared at pH 2. The Langmuir and Freundlish isotherms were utilized to analyze the adsorption capacity of the HEA/AMPS copolymer hydrogels.

The linear form of the Langmuir adsorption isotherm equation (Langmuir 1918) is:

$$\frac{C\mathrm{e}}{Q\mathrm{e}} = \frac{1}{\mathrm{Ke}Q\max} + \frac{Ce}{Q\max} \quad (2)$$

where Ce is the equilibrium concentration of adsorbate (milligram per liter), Qe is the amount of the heavy metal ion adsorbed by the hydrogel at equilibrium (milligram per gram), Ke is the Langmuir equilibrium constant (liter per milligram), and Qmax is the amount of adsorbate required to cover a monolayer (milligram per gram).

The Freundlich adsorption isotherm equation (Freudlich 1907) is:

$$\mathrm{Ln}Q = \mathrm{LnK} + \frac{1}{n}\mathrm{LnCe} \quad (3)$$

where Q is the amount of adsorbate adsorbed per unit weight (milligram per gram), K is the Freundlich equilibrium constant (liter per milligram), n is the Freundlich equilibrium constant, and Ce is the equilibrium concentration of heavy metal ions (milligram per liter).

The studies on adsorption kinetics were conducted with an initial feed concentration of 200 mg L^{-1} at pH 6 and

ambient temperature. The concentrations of each heavy metal ion in the solutions were analyzed for a series of time points (0, 0.25, 0.5, 1, 2, 3, 4, 6, 8, 10, 21, 24, 48, and 72 h).

The single-component heavy metal ion concentrations adsorbed per unit mass of hydrogel (mg metal ion, per gram dry hydrogel) were calculated using the expression:

$$Q = \frac{(C - C_0) \times V}{m} \quad (4)$$

where Q is the amount of heavy metal ion adsorbed (milligram per gram), C_0 and C are the concentrations of the metal ions in the aqueous phase before and after the treatment (milligram per liter), V is the volume of the aqueous phase (liter), and m is the amount of dry hydrogel (gram).

The pseudo-first-order and pseudo-second-order equations were adopted to test the adsorption capability and to understand the adsorption process better. The pseudo-first-order equation is as follows:

$$\mathrm{Ln}\,(\mathrm{Qe} - \mathrm{Qt}) = -k_1 t + \mathrm{LnQe} \quad (5)$$

where Qt (milligram per gram) is the adsorption amount at time t (minute), Qe (milligram per gram) is the adsorption capacity at adsorption equilibrium, and k_1 is the kinetics rate constant for the pseudo-first-order equation (per minute).

The pseudo-second-order equation is as follows:

$$\frac{\mathrm{t}}{Q\mathrm{t}} = \frac{\mathrm{t}}{Q\mathrm{e}} + \frac{1}{\mathrm{k}_2 Qe^2} \quad (6)$$

where Qt (milligram per gram) is the adsorption amount at time t (min), Qe (milligram per gram) is the adsorption capacity at adsorption equilibrium, and k_2 is the kinetics rate constant for the pseudo-second-order equation (gram per milligram per minute).

Multicomponent heavy metal ion adsorption

The experiment of multicomponent heavy metal ion adsorption of Pb^{2+}, Cd^{2+}, Cu^{2+}, Cr^{3+}, and Fe^{3+} by copolymer hydrogel was performed at room temperature for 48 h at pH 6. The components of the multicomponent heavy metal ion solutions are listed in Table 2. The concentrations were either 500 or 200 mg L^{-1}. Furthermore, this experiment was studied with the hydrogel component experimental group A-2-c (Table 1) for convenience.

Multicomponent heavy metal ion concentrations adsorbed per unit mass of hydrogel (millimoles metal ion per gram dry hydrogel) were calculated by:

$$Q_x = \frac{(C - C_0) \times V/M}{m} \quad (7)$$

where Q_x is the amount of heavy metal ion adsorbed (millimoles per gram), C_0 and C are the concentrations of metal ions in aqueous phase before and after treatment (milligram per liter), V is the volume of the aqueous phase (liter), M is the molecular weight of the corresponding heavy metal ion (gram per mole), and m is the amount of dry hydrogel (gram).

Table 2 Components of multicomponent heavy metal ions solutions (milligram per liter)

Items	Pb^{2+}	Cd^{2+}	Cu^{2+}	Cr^{3+}	Fe^{3+}
Pb + Cd	500	500			
Pb + Cu	500		500		
Pb + Fe	500				500
Cd + Cu		500	500		
Cd + Fe		500			500
Fe + Cr				500	500
Pb + Cu + Cd	200	200	200		
Pb + Cd + Cr	200	200		200	
Pb + Cd + Fe	200	200			200
All	200	200	200	200	200

Results

Characteristics of HEA/AMPS copolymer hydrogels

Morphology

Figure 1 shows the SEM morphologies of the HEA/AMPS copolymer hydrogel. It demonstrates that the microstructure of the HEA/AMPS copolymer hydrogel had a three-dimensional network supported by crack-like and thick crystal HEA/AMPS copolymer walls. Furthermore, Fig. 1a distinctly reveals that the HEA/AMPS copolymer hydrogel adsorbent area was very coarse and irregularly shaped; whereas Fig. 1b demonstrates a smooth surface with some micropores finely dispersed inside the copolymer hydrogel. The size of the micropores ranged from approximately 10–50 μm, and they were interspersed on the surface.

The XPS spectrum of the surface characteristics for the HEA/AMPS copolymer hydrogel is shown in Fig. 2. The characteristic peaks of C1s, N1s, O1s, and S2p for the copolymer hydrogel were observed clearly at BE of 284, 399, 531, and 168 eV, respectively (Zheng et al. 2011).

FTIR

The FTIR spectrum of the AMPS monomer is shown in Fig. 3a. The strong peaks around 2,985.3, 1,245.8, and 1,087.7 cm^{-1} arose from the deformation vibration of –NH, $–SO_2$ symmetrical stretching vibration, and $–SO_2$ asymmetrical stretching vibration, respectively. The broad absorption

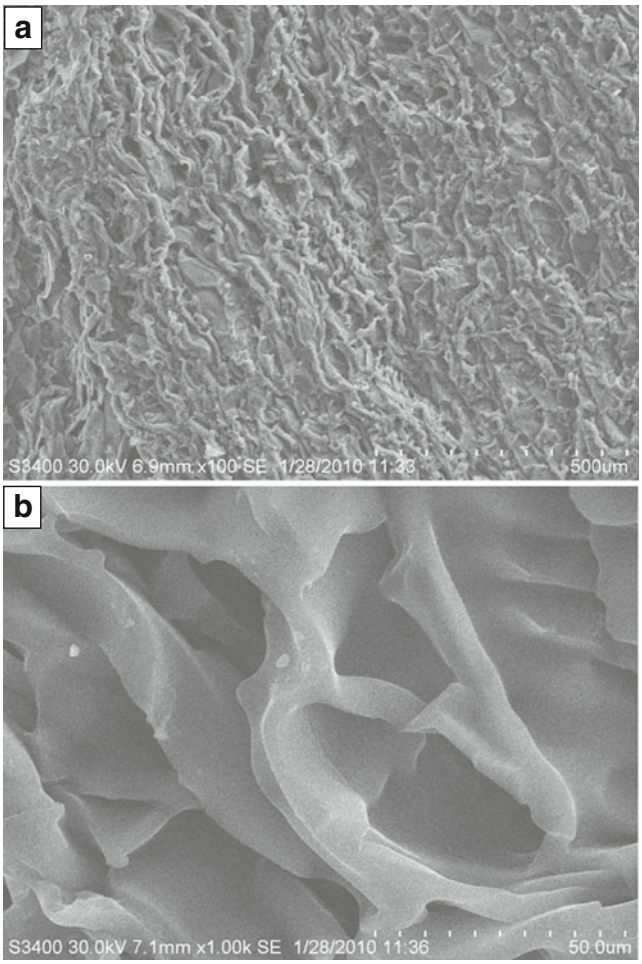

Fig. 1 SEM image of HEA/AMPS copolymer hydrogel with 70 wt% deionized water (the hydrogel components experimental group A-2-c) at two different magnifications: **a** ×100, **b** ×1,000

band around 1,700–1,600 cm^{-1}, which had two typical peaks at 1,670.0 and 1,614.2 cm^{-1}, was ascribed to the existence of amide I, amide II, and amide III of the $-CO_2NH-$ group (Rivas and Castro 2003).

Figure 3b shows the FTIR spectra of the HEA monomer. The strong peaks around 3,430.8, 2,954.5, and 1,724.1 cm^{-1} were due to the stretching vibration of –OH, deformation

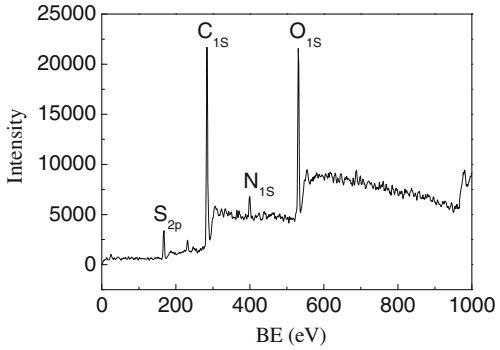

Fig. 2 XPS of HEA/AMPS copolymer hydrogel group A-2-c

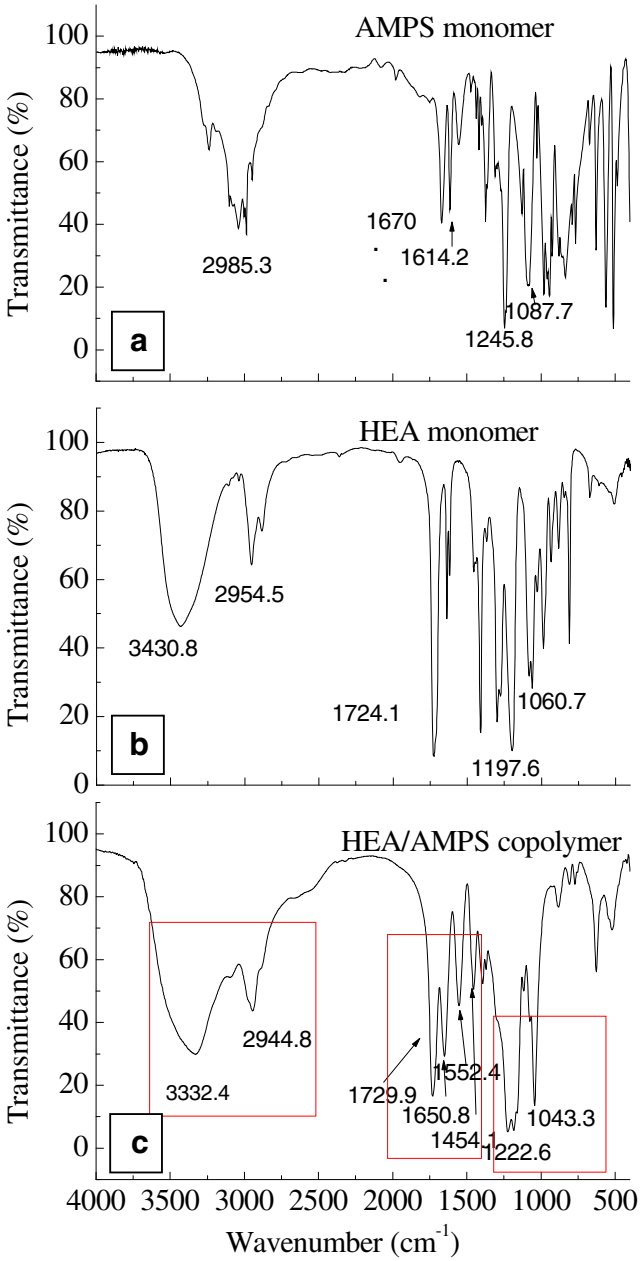

Fig. 3 FTIR spectra of **a** AMPS monomer, **b** HEA monomer, and **c** HEA/AMPS copolymer

vibration of C–H, and stretching vibration of –COO–, respectively (Bozkurt et al. 2003). Several typical strong peaks, including those at 1,197.6 and 1,060.7 cm^{-1}, were observed in the broad absorption band within 1,300–1,000 cm^{-1}.

As seen in Fig. 3c, the broad absorption band within 3,600–2,900 cm^{-1} was ascribed to the existence of –OH, C–H, and –NH groups. The strong peaks around 3,332.4 and 2,944.8 cm^{-1} were due to the stretching vibration of –OH and the overlapping peaks of –NH and C–H groups, respectively. Four strong peaks existed in the broad absorption band around 2,000–1,400 cm^{-1}. The strong peaks

around 1,729.9, 1,650.8, 1,552.4, and 1,454.1 cm^{-1} were ascribed to the stretching vibration of –COO–, stretching vibration of C=O (amide I), flexural vibrations of N–H (amide II), and stretching vibration C–N (amide III), respectively. In the broad absorption band around 1,300–1,000 cm^{-1}, the typical strong peaks around 1,222.6 and 1,043.3 cm^{-1} were due to the symmetrical and asymmetrical stretching vibration of $–SO_2$, respectively (Bozkurt et al. 2003; Rivas and Castro 2003).

TGA

The general characteristics of the HEA/AMPS copolymer hydrogel thermograms with different compositions are demonstrated in Fig. 4. The primary thermograms of all hydrogel experimental groups had typical sigmoidal shapes. The weight loss was nearly constant when temperatures were higher than 450 °C. Three characteristic weight loss peaks were observed; viz. around 20–210 °C, 210–340 °C, and 340–450 °C.

The effects of AMPS and HEA molar ratios on the weight loss of the copolymer hydrogels are shown in Fig. 4a. In the weight loss peaks within the range of 20–450 °C, the copolymer hydrogel weight loss increased as the AMPS content increased when *n* (AMPS)/*n* (HEA)<1:1 (experimental groups A-2-a, A-2-b, and A-2-c). However, the TGA curve of the experimental group A-2-d ((AMPS): *n* (HEA)=1:1) almost overlapped with the experimental group A-2-a ((AMPS)/*n* (HEA)=1:9) in the first peak (20–210 °C). In the second peak (210–340 °C), the weight loss performance of group A-2-d was between group A-2-a and group A-2-b ((AMPS)/*n* (HEA)=1:4). In the third peak (340–450 °C), the weight loss in group A-2-d was less than that in group A-2-c ((AMPS)/*n* (HEA)=2:3). However, when the temperature was more than 450 °C, group A-2-d maintained the highest weight (approximately 30 %).

Figure 4b showed the effect of the volume ratio on weight loss of the copolymer hydrogels. All TGA curves were almost overlapping, showing that the effect of the water volume ratios on the weight loss of the copolymer hydrogel was negligible. When the temperature was higher than 450 °C, group A-3-c retained the highest weight (approximately 20 % moisture).

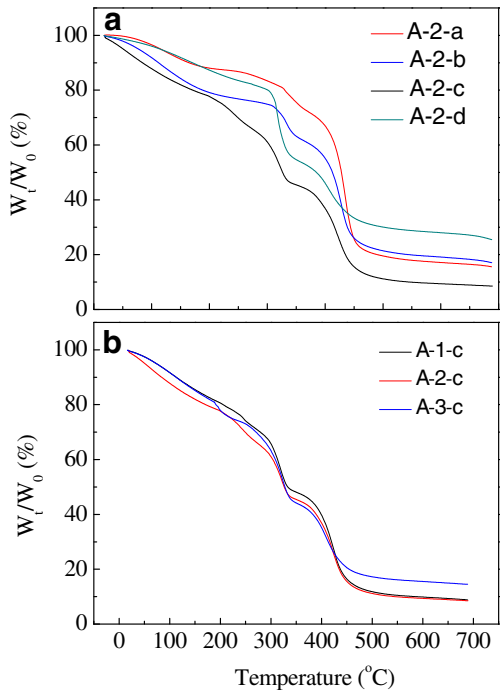

Fig. 4 TGA curves of HEA/AMPS copolymer hydrogels: **a** constant water volume ratios with different AMPS and HEA molar ratios **b** constant AMPS and HEA molar ratios with different water volume ratios. Wt and W_0 represented the weight of the HEA/AMPS copolymer hydrogel after and before TGA treatment

Swelling

The EDS values of the copolymer hydrogels were affected strongly by the AMPS content (Fig. 5). Increasing AMPS contents increased the EDS values. The EDS values increased from 1.4, 6.1, and 2.5 to 4.5, 26.1, and 12.4 by increasing the AMPS content (10–50 %) for water volume ratios of 80, 70, and 60 %, respectively. The 70 % water volume ratio yielded the best EDS effect, and the experimental group A-2-d (*n* (AMPS)/*n* (HEA)=1:1) achieved the optimum swelling capacity.

Single-component heavy metal ion adsorption

Effect of different hydrogel compositions

The effects of HEA/AMPS copolymer hydrogel composition on the adsorption of Pb^{2+}, Cr^{3+}, Cd^{2+}, Cu^{2+}, and Fe^{3+}

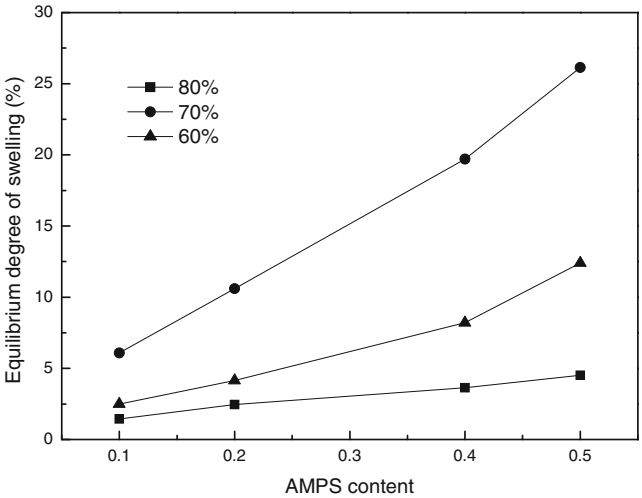

Fig. 5 Equilibrium degree of swelling of HEA/AMPS copolymer hydrogels

are shown in Fig. 6. In general, increasing AMPS content increased the adsorption effect of the copolymer hydrogel. However, the adsorption effect of Cr^{3+} decreased with the increase of the AMPS content from 0.4 to 0.5 for both 60 and 70 % water volume ratios (Fig. 6b). On the other hand, the water volume ratio in the copolymer hydrogel also affected strongly the heavy metal ion adsorption capacity with constant AMPS content. In Fig. 6a, the 70 % water volume ratio achieved an optimal Pb^{2+} adsorption effect when the AMPS content was less than 0.5. The 60 % water volume ratio achieved the optimal Pb^{2+} adsorption effect for 0.5 AMPS content. The 80, 70, and 70 % water volume ratios achieved the optimal Cr^{3+}, Cd^{2+}, and Cu^{2+} adsorption effects, respectively, at various AMPS contents (Fig. 6b–d). The water volume ratio of 60 % achieved the best Fe^{3+} adsorption effect when the AMPS content was less than 0.5 (Fig. 6e). The optimal Pb^{2+} adsorption effect for 0.5 AMPS content was achieved with a 70 % water volume ratio. Therefore, the 70 % water volume ratio with 0.5 AMPS content (*n* (AMPS)/*n* (HEA)=1:1), namely, the experimental group A-2-d, achieved the best effects for single-component metal adsorptions, when all heavy metal ions were considered.

Effect of pH

The effects of pH on the adsorption capacity of HEA/AMPS copolymer hydrogel are shown in Fig. 7. Generally, increasing pH (from pH 1 to 6) increased the adsorption levels of the copolymer hydrogel for Pb^{2+}, Cr^{3+}, Cd^{2+}, and Cu^{2+}, which increased from 22 to 175, 51 to 131, 69 to 92, and 102 to 160 mg g^{-1}, respectively. Yildi et al. (2010) reported a similar result, showing that the copolymer hydrogel was pH sensitive. The adsorption of Pb^{2+} underwent a rapid increase as pH rose from 1 to 6. Cu^{2+}, Cd^{2+}, and Cr^{3+} adsorption amounts barely increased with the increase of pH from 1 to 2. However, the adsorption of Cd^{2+} and Cr^{3+} slightly increased as pH varied from 2 to 4, whereas Cu^{2+} increased significantly. Cr^{3+} and Cu^{2+} adsorption amounts both increased strongly, with pH rising from 5 to 6, after slightly decreasing in the pH range 4–5. Cd^{2+} adsorption amount maintained rapid growth, with the pH increasing from 4 to 6.

The adsorption amount of Fe^{3+} was distinctive. An obvious decrease from 147 to 60 mg g^{-1} was observed with the increase of pH from 2 to 3, after a very strong increase from 26 to 147 mg g^{-1} with the increase of pH from 1 to 2. The adsorption amount of Fe^{3+} was 60 to 80 mg g^{-1}, or nearly constant, at pH 3–7. These results were similar to those reported by Kok Yetimoglu et al. (2007).

The maximum adsorption contents of heavy metal ions were achieved at Ph 6 for Pb^{2+}, Cr^{3+}, Cd^{2+}, and Cu^{2+}. The best Fe^{3+} adsorption effect was observed at pH 2. When considering all metal ions, the optimal adsorption effects of heavy metal ions were at pH 6.0.

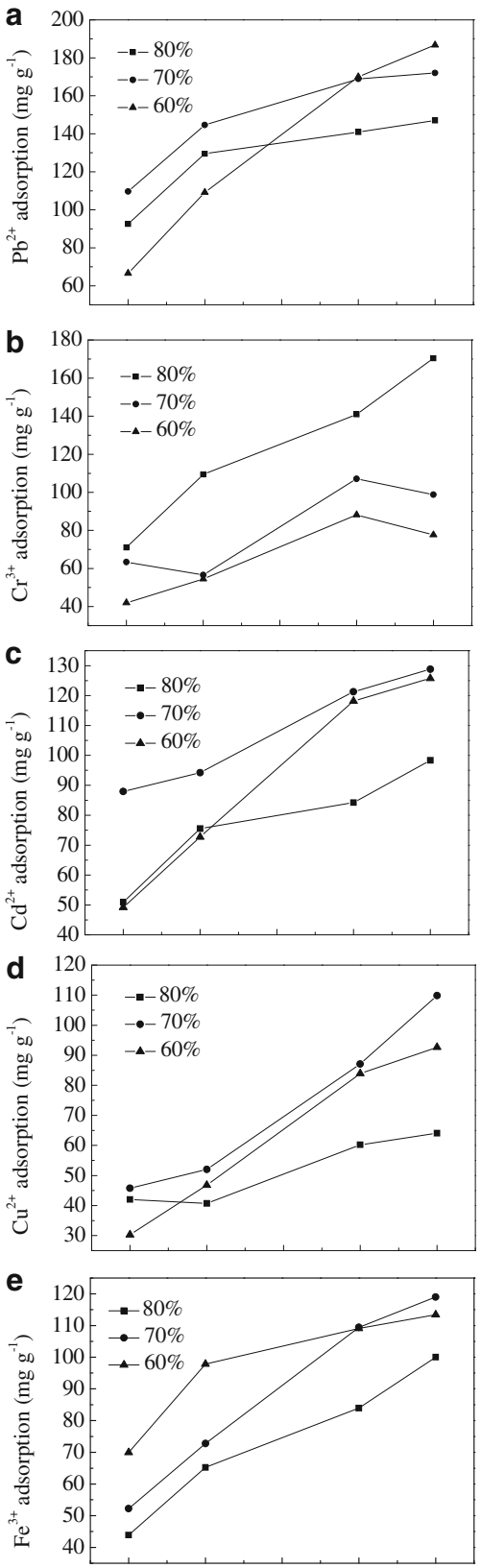

Fig. 6 Adsorption of heavy metal ions: **a** Pb^{2+}, **b** Cr^{3+}, **c** Cd^{2}+, **d** Cu^{2}+, and **e** Fe^{3+}

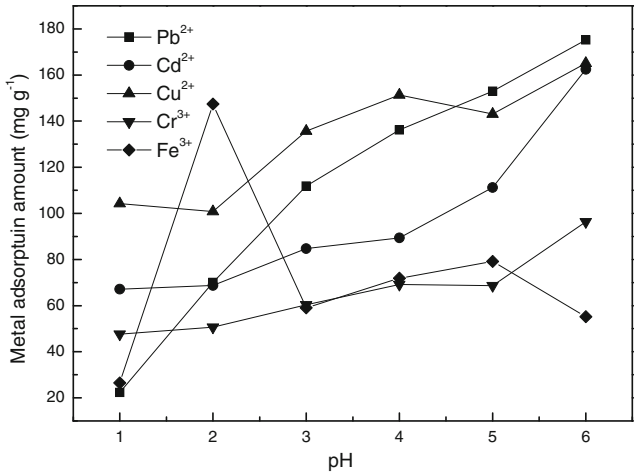

Fig. 7 Effect of pH on adsorption of heavy metal ions

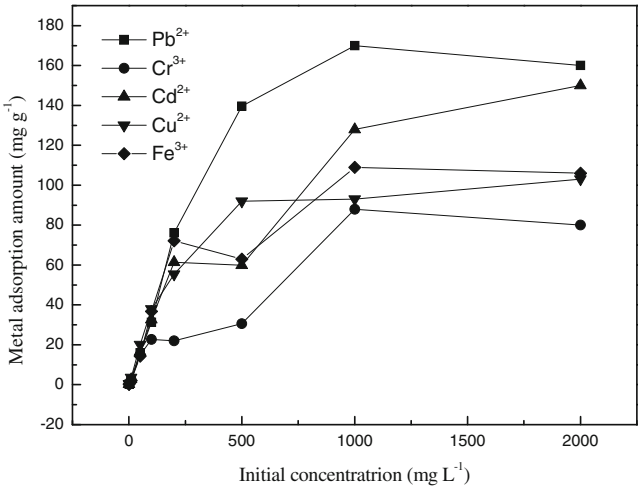

Fig. 9 Effect of initial heavy metal ion concentration on adsorption of heavy metal ions

Effects of temperature

Temperature clearly affected the adsorption (Fig. 8). In general, the adsorption amounts of Pb^{2+}, Cd^{2+}, Cu^{2+}, Cr^{3+}, and Fe^{3+} decreased as the temperature increased from 15 to 40 °C. Compared with the others, the adsorption of Pb^{2+} was very high at 15 °C, but declined very rapidly until 30 °C. The adsorption amounts of Cu^{2+}, Cd^{2+}, Cr^{3+}, and Fe^{3+} barely changed with temperature increases from 15 to 30 °C. However, the adsorption amounts rapidly decreased thereafter. The optimal temperature for adsorption of all the heavy metal ions was 15 °C.

Isotherm

Effect of initial heavy metal ion concentration The effects of the initial heavy metal ion concentrations on the adsorption capacity are displayed in Fig. 9. The adsorption amounts of Pb^{2+}, Cd^{2+}, Cr^{3+}, and Fe^{3+} increased rapidly with increasing initial metal ion concentration from 1 to 1,000 mg L^{-1}, after which they remained constant. The increasing initial ion concentration from 1 to 500 mg L^{-1} increased the adsorption amount for Cu^{2+}, and then an equilibrium level at a maximum concentration of 500 mg L^{-1} was reached.

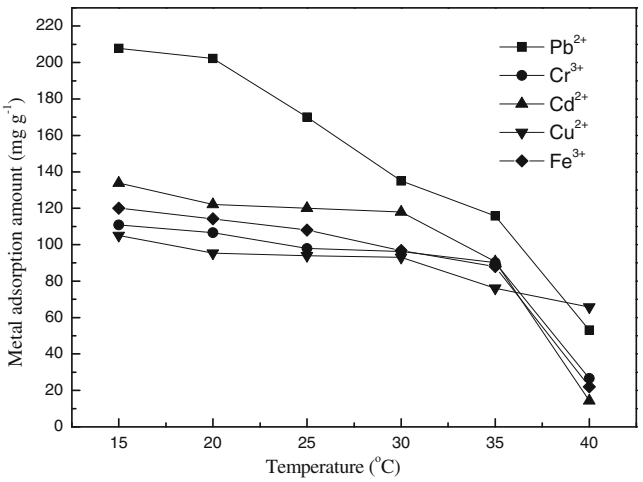

Fig. 8 Effect of temperature on adsorption of heavy metal ions

Langmuir and Freundlish adsorption isotherms The Langmuir adsorption isotherm (Eq. 2) and Freundlish adsorption isotherm (Eq. 3) were used to analyze the adsorption capacities of the HEA/AMPS copolymer hydrogels (Fig. 10). The parameters of the adsorption isotherm models are given in Table 3. The R^2 for all heavy metal ions in the Langmuir adsorption isotherm were consistently larger than that for the Freundlish adsorption isotherm. The values of the Freundlish adsorption isotherm constant n were 1.292, 1.330, 1.345, 1.684, and 1.432 for Pb^{2+}, Cr^{3+}, Cd^{2+}, Cu^{2+}, and Fe^{3+}, respectively. All the values were within 0–10, indicating that the sorption of heavy metal ions by HEA/AMPS copolymer hydrogels was favorable (Abdel-Halim and Al-Deyab 2011).

The *Qmax* in the Langmuir adsorption isotherm (Eq. 2) model indicated that the adsorption capacity of the copolymer hydrogel was high. The maximum sorption capacities for Pb^{2+}, Cr^{3+}, Cd^{2+}, Cu^{2+}, and Fe^{3+} were 208, 103, 167, 105, and 123 mg g^{-1}, respectively (Table 3).

Kinetics

Contact time The effects of contact time on the adsorption amounts are shown in Fig. 11. The metal adsorption amounts of Pb^{2+}, Cd^{2+}, Cu^{2+}, and Fe^{3+} rose quickly with increasing contact time from 1 to 24 h, after which the amounts of Pb^{2+}, Cd^{2+}, Cu^{2+} and Fe^{3+} leveled off. For Cr^{3+}, the increment in contact time from 1 to 5 h increased the

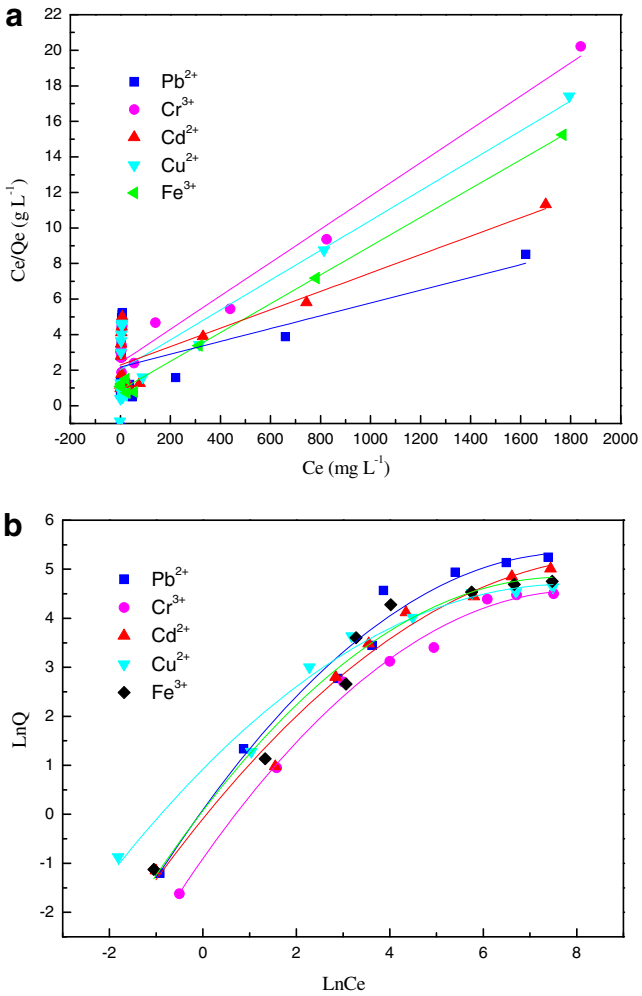

Fig. 10 **a** Langmuir adsorption isotherm and **b** Freundlich adsorption isotherms

adsorption amount, and an equilibrium level was achieved at 5 h.

The pseudo-first-order and the pseudo-second-order equations The pseudo-first-order equation (Eq. 5) and the pseudo-second-order equation (Eq. 6) were utilized to characterize the adsorption experiment, as shown in Fig. 12. The parameters of the equations are listed in Table 4. The R^2 for all kinds of heavy metal ions in the pseudo-second-order equation were evidently larger than that for the pseudo-first-order equation. The pseudo-second-order equation described the adsorption process well.

Multicomponent heavy metal ion adsorption

The multicomponent heavy metal ion adsorption effects are demonstrated in Fig. 13. The adsorption capacities of all metal ions decreased under competitive conditions compared with the respective single-component heavy metal ion adsorption levels.

The experimental groups with two-component metal ion combination showed different results. Cd^{2+} influenced the adsorption capacity of Pb^{2+} strongly, and the adsorption amount in the Pb^{2+}+Cd^{2+} group was decreased by 45 %. Nevertheless, the Cd^{2+} adsorption amount only decreased slightly. In the Cu^{2+} and Cd^{2+} group, the adsorption capacities of Cu^{2+} and Cd^{2+} declined by 47 and 52 %, respectively. In the Cu^{2+} and Pb^{2+}, Fe^{3+} and Cr^{3+}, Fe^{3+} and Cd^{2+}, and Fe^{3+} and Pb^{2+} groups, the adsorption capacity of Pb^{2+} declined a little more than Cu^{2+}, Fe^{3+} declined a little more than Cr^{3+}, Fe^{3+} declined a little less than Cd^{2+}, and Fe^{3+} declined a little less than Pb^{2+}.

Similar trends were evident in solutions containing three kinds of heavy metal ions. In the Pb^{2+}, Cu^{2+}, and Cd^{2+} combination, the adsorption capacities decreased to 65, 43, and 63 %, respectively. In the Pb^{2+}, Cd^{2+}, and Fe^{3+} group, the adsorption capacities decreased to 82, 72, and 23 %, respectively. Finally, with all five heavy metal ions combined, the adsorption capacities of Pb^{2+}, Cu^{2+}, Cd^{2+}, Cr^{3+}, and Fe^{3+} dropped to 98, 57, 62, 12, and 49 %, respectively.

Adsorption mechanism

The chemical structures of the HEA/AMPS copolymer hydrogels (experimental group A-2-c) were characterized by FTIR before and after the adsorption treatment (Fig. 14). Three peak areas (first absorption band around 3,600–2,900 cm^{-1}, second absorption band with strong peaks at 1,729.9, 1,650.8, 1,552.4, and 1,454.1 cm^{-1}, and third absorption band around 1,300–1,000 cm^{-1}) were

Table 3 Parameters of the adsorption isotherm models

Ion	Langmuir			Freundlich		
	Ke (L mg^{-1})×10^{-3}	*Q*max (mg g^{-1})	R^2	*n*	*K* (L mg^{-1})	R^2
Pb^{2+}	6.96	208	0.992	1.292	1.515	0.908
Cr^{3+}	4.77	103	0.982	1.330	0.676	0.926
Cd^{2+}	4.90	167	0.987	1.345	1.189	0.932
Cu^{2+}	1.67	105	0.998	1.684	2.535	0.899
Fe^{3+}	9.25	123	0.996	1.432	1.493	0.885

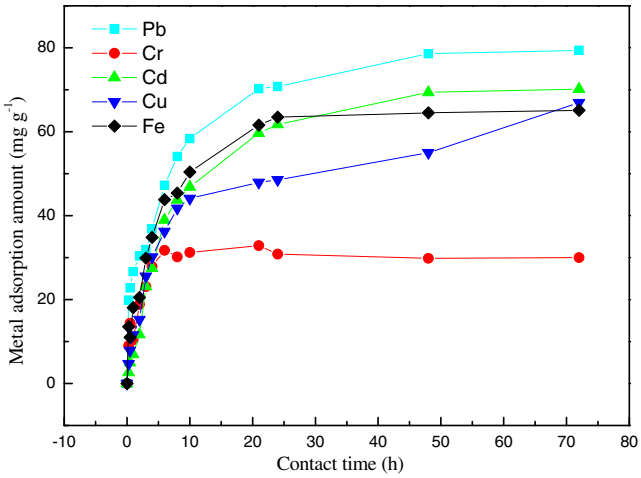

Fig. 11 Effect of contact time on adsorption of heavy metal ions

involved in the adsorption mechanism of the copolymer hydrogel, as mentioned in "FTIR" and "FTIR" sections. The variation trends before and after treatment for the five

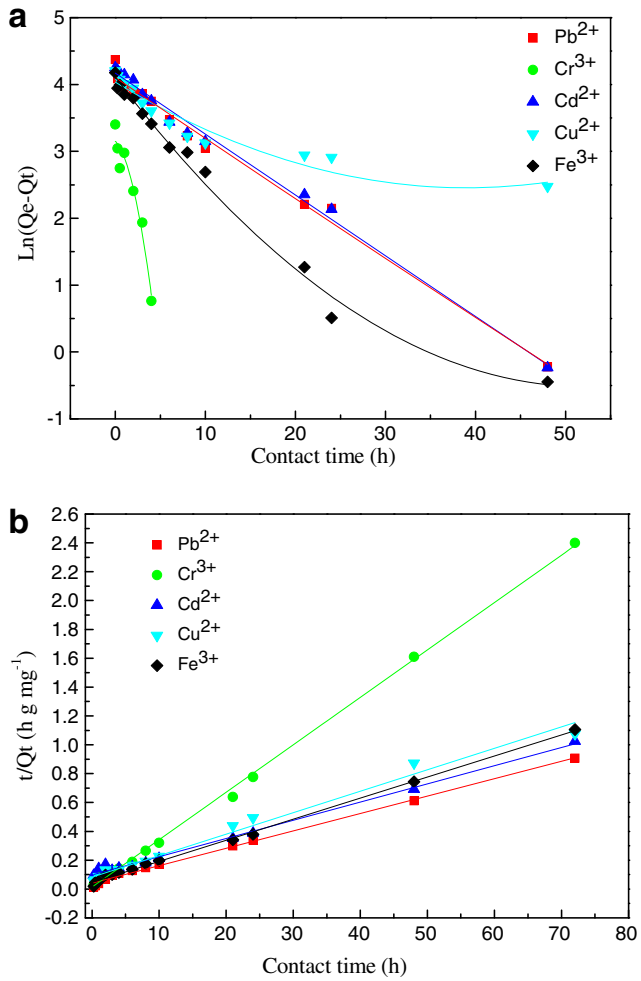

Fig. 12 **a** The pseudo-first-order equation and **b** the pseudo-second-order equations

metal ions were similar. The first and second peak areas were slightly strengthened after adsorption. The shoulder of the third peak area around 1,223–1,160 cm^{-1} was a little weakened, with the peak changing from around 1,043–1,039 cm^{-1} (Fig. 14).

Discussions

Characteristics of the copolymer hydrogel

Morphology

The surface morphology of the copolymer hydrogel was beneficial for permeation due to coarse, irregularly shaped pores in the hydrogel (Fig. 1). This feature increased the accessibility of the reactive functional groups within the polymeric network (Abdel-Halim et al. 2011). Zheng et al. (2011) reported similar results demonstrating that the adsorption equilibrium of Ni^{2+} was achieved more quickly due to the accessibility of reactive functional groups in the copolymer hydrogel. The porous structure might also be related to higher copolymer swelling capacity (El-Hag Ali et al. 2003; Pourjavadi and Barzegar 2009; Cao et al. 2010).

FTIR

The absorption bands in the FTIR spectra of HEA/AMPS copolymers at around 3,332.4 and 2,944.8 cm^{-1} (Fig. 3c) resulted from the HEA with stretching vibration of –OH (3,430.8 cm^{-1} in Fig. 3b), the overlapping peaks of –NH from AMPS (2,985.3 cm^{-1} in Fig. 3a), and C–H from HEA (2,954.5 cm^{-1} in Fig. 3b), respectively (Bozkurt et al. 2003; Rivas and Castro 2003). The strong peaks around 1,729.9 cm^{-1} (Fig. 3c) were ascribed to the HEA with stretching vibration of –COO– (1,724.1 cm^{-1} in Fig. 3b; Bozkurt et al. 2003). The strong peaks around 1,650.8, 1,552.4, and 1,454.1 cm^{-1} (Fig. 3c) were due to amide I, amide II, and amide III from AMPS (absorption band around 1,700–1,600 cm^{-1} in Fig. 3a), respectively (Rivas and Castro 2003). In Fig. 3c, the typical strong peaks were around 1,222.6 and 1,043.3 cm^{-1} from the AMPS with symmetrical (1,245.8 cm^{-1} in Fig. 3a) and asymmetrical stretching vibration of $–SO_2$ (1,087.7 cm^{-1} in Fig. 3a), respectively (Rivas and Castro 2003).

Furthermore, the characteristic absorption bands in the FTIR spectrum of AMPS (Fig. 3a) and HEA (Fig. 3b) monomers were weakened by other absorption bands, which means that the reactive functional groups of AMPS (such as –NH and $–SO_2$) and HEA (such as C–H and –COO–) took part in the copolymerization reactions. The results were similar to those of Zheng et al. (2011). The HEA had been grafted firmly on the backbone of AMPS during the

Table 4 Parameters of adsorption kinetics models

Item	Pseudo-first-order model			Pseudo-second-order model		
	k_1 (min^{-1})	Qe (mg g^{-1})	R^2	k_2 (g mg^{-1} min^{-1})×10^{-3}	Qe (mg g^{-1})	R^2
Pb^{2+}	0.090	60.220	0.991	3.58	82.645	0.996
Cr^{3+}	0.562	27.952	0.918	8.33	30.395	0.998
Cd^{2+}	0.091	64.651	0.992	1.63	79.365	0.995
Cu^{2+}	0.036	48.010	0.787	2.68	67.114	0.985
Fe^{3+}	0.103	46.628	0.939	5.31	68.027	0.997

copolymerization reaction period. This result was verified by the XPS spectra of the copolymer hydrogel.

TGA

Generally, the thermal stability increased as the AMPS content decreased with a constant water volume ratio of 70 wt% (Fig. 4a). The A-2-a group achieved the highest thermal stability at temperatures higher than 450 °C. These phenomena were explained by the theory that the weight loss peaks at 20–210, 210–340, and 340–450 °C resulted from the losses of copolymer hydrogel water components, $–SO_2$ from AMPS, and breaking of the primary chemical bond of the copolymer hydrogel, respectively (El-Hag Ali et al. 2003). Meanwhile, in the temperature range 20–450 °C, the thermal stability of the A-2-d group, which had the highest AMPS content (Table 1), was not much lower than the A-2-a group. Kok Yetimoglu et al. (2007) reported similar results suggesting that the thermal stability of the prepared hydrogel increased as more stable moiety content was achieved in the components of the hydrogel. The water content in the copolymer hydrogel was almost lost when the weight loss stabilized. Group A-2-d represented the best thermal stability with a 30 % residual weight.

The thermal stability was nearly irrelevant to the water volume ratios in the hydrogel components with a constant AMPS content (Fig. 4b). However, group A-3-c achieved the highest weight reserve (around 20 %) when the weight loss was constant due to the lower water volume ratio (Table 1).

Thus, the HEA/AMPS copolymer hydrogel with a higher AMPS content showed a slightly lower thermal stability. Group A-2-d was the optimal copolymer hydrogel because the thermal stability and weight reserve were simultaneous in a broad temperature range (20–700 °C).

Swelling

The increasing AMPS content produced increasing hydrophilicity of the copolymer hydrogel because AMPS is a hydrophilic polymer. The morphology of the HEA/AMPS copolymer hydrogel (Fig. 1) showed that the copolymer hydrogel had a porous structure due to the pores in the AMPS. These results were similar to those of Rueda et al. (2003). The pores in the HEA/AMPS copolymers were regions of water permeation and interaction sites of external stimuli with incorporated hydrophilic groups (Pourjavadi and Barzegar 2009). Therefore, the porous structure was

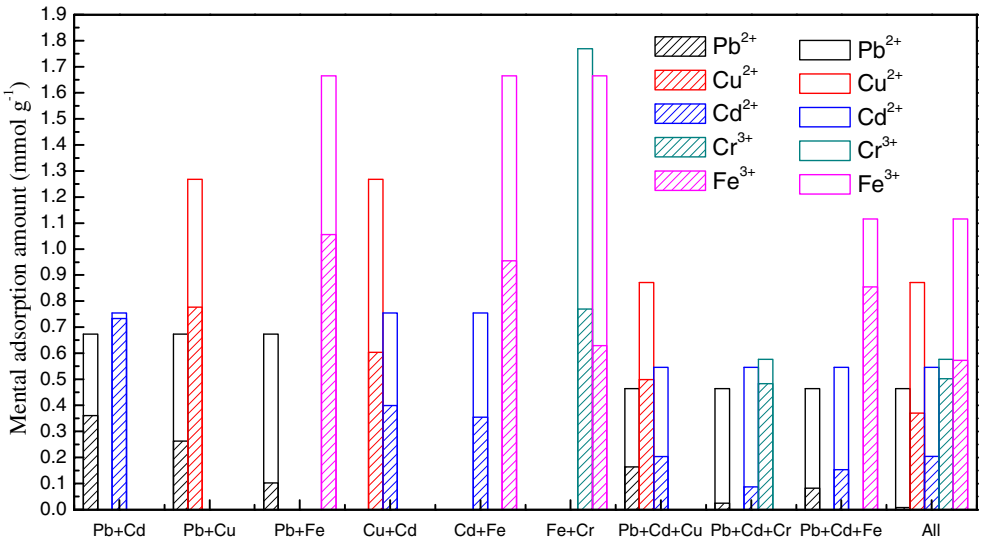

Fig. 13 Multicomponent heavy metal ions adsorption capacities (*oblique lined area* single component adsorption, *blank area* multicomponent adsorption)

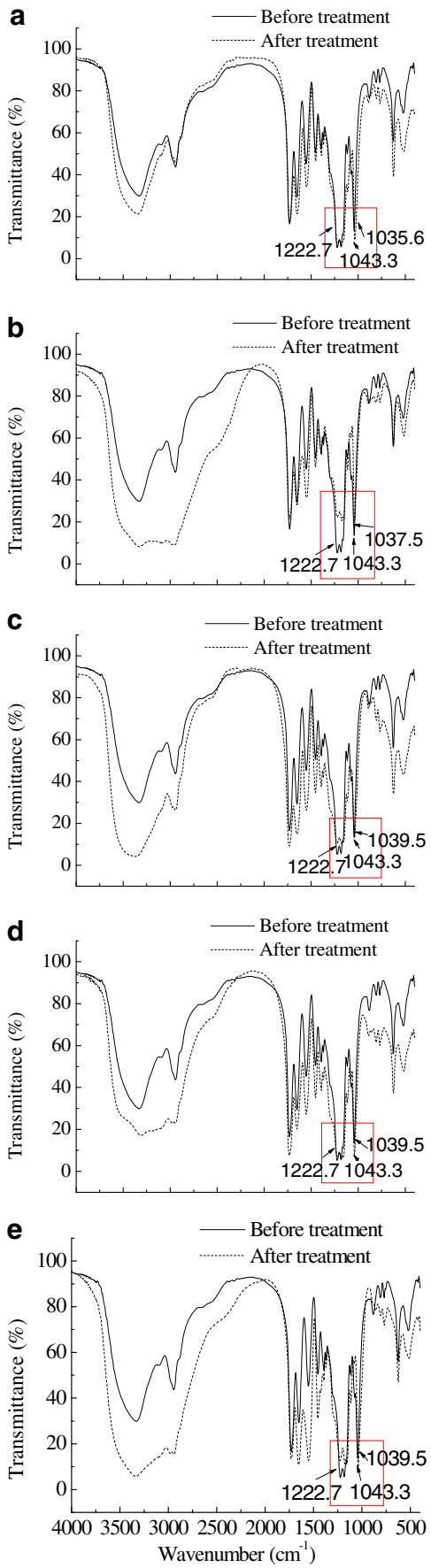

◀ **Fig. 14** FTIR spectra of the copolymer hydrogel before and after treatment: **a** Pb^{2+}, **b** Cr^{3+}, **c** Cd^{2}+, **d** Cu^{2}+, and **e** Fe^{3+}

the predominant reason for the high swelling capacity of the copolymer hydrogel. Consequently, the hydrogel porosity and absorptive capacity of the copolymer hydrogels for polar liquids depend on and increase with the AMPS content (Kok Yetimoglu et al. 2007). Experimental group A-2-d, which possessed the highest AMPS content with a moderate water volume ratio (Table 1), achieved the optimum swelling capacity.

Single-component heavy metal ion adsorption

Effect of different compositions of hydrogels

AMPS was responsible for heavy metal ion adsorption. Essawy and Ibrahim (2004) reported similar results suggesting that a porous structure of AMPS was beneficial for heavy metal ion accessibility to the reactive functional groups of the polymeric networks. However, Cr^{3+} adsorption decreased with the AMPS content increasing from 0.4 to 0.5 at both 60 and 70 % water volume ratios (Fig. 6b). This phenomenon arose from the different adsorption mechanisms of Cr^{3+} compared with the other heavy metal ions (Kasgoz et al. 2003). The function groups for Pb^{2+}, Cd^{2+}, Cu^{2+}, and Fe^{3+} adsorption came from AMPS, whereas that for Cr^{3+} was due to the C=O group from HEA (Fig. 3b). Thus, the Cr^{3+} adsorption effect declined when the AMPS content increased to a certain level and the HEA content was too low to provide sufficient C=O groups for Cr^{3+} adsorption. Moreover, the ratio of water volume with constant AMPS content determined the pore size and functional group distribution of the copolymer hydrogel.

Effect of pH

The adsorption capacity of heavy metal ions evidently decreased at lower pH (Fig. 7). This phenomenon was due to the theory that the reactive functional groups within the network of copolymer hydrogel were protonated at lower pH. The metal ions had to compete with the proton for absorbency and the protonated functional groups hindered the interaction between the adsorbent and heavy metal cations (Huang et al. 2007; Ijagbemi et al. 2010). In addition, the poor performance of Fe^{3+} adsorption at pH>2 was due to the insolubility of the heavy metal hydroxide (Kok Yetimoglu et al. 2007).

Effect of temperature

Temperature is an important factor influencing heavy metal ion adsorption by the copolymer hydrogel (Yildi et al.

2010). In the present research, the HEA/AMPS copolymer hydrogel showed a high adsorption capacity for the heavy metal ions at lower temperature (Fig. 8), indicating that the adsorption process of heavy metal ions is an exothermic reaction.

Isotherm

In general, an increase in the metal ion concentration accelerated the diffusion of the metal ion into the polymeric network because of the increased driving force of the concentration gradient (Zheng et al. 2011). In addition, the equilibrium level (Fig. 9) demonstrated that the maximum load capacity of Pb^{2+}, Cd^{2+}, Cr^{3+}, and Fe^{3+} was 1,000 mg L^{-1}, whereas that for Cu^{2+} was 500 mg L^{-1}.

The Langmuir adsorption isotherm was a better mathematical fit for equilibrium data than the Freundlish adsorption isotherm (Table 3). Therefore, the adsorption process of HEA/AMPS copolymer hydrogel for heavy metal ions was a monolayer adsorption process, which occurred at specific homogeneous sites on the adsorbent (Abdel-Halim and Al-Deyab 2011).

Kinetics

The adsorption rates were rapid and the adsorption equilibrium was achieved within 24 h for Pb^{2+}, Cd^{2+}, Cu^{2+}, and Fe^{3+}, and 5 h for Cr^{3+} (Fig. 11). These phenomena were due to the superhydrophilic polymeric network and an abundance of reactive functional groups in the HEA/AMPS copolymer hydrogel (Zheng et al. 2011). These rapid adsorption rates were consistent with predictions from SEM (Fig. 1).

The Cr^{3+} adsorption rate was much larger than that of the other heavy metal ions (parameter k_2 in Table 4). This finding indicated that the adsorption process was very fast, and that it may be dominated by a chemical adsorption phenomenon (Zheng et al. 2011). The HEA/AMPS copolymer hydrogel was proven adsorbent with high adsorption capacity and fast adsorption rate for heavy metal ions.

Multicomponent heavy metal ion adsorption

The priority order in multicomponent adsorption was Cr^{3+}>Fe^{3+}>Cu^{2+}>Cd^{2+}>Pb^{2+}. The adsorption capacity of Cr^{3+} reached the maximum before the other ions because its adsorption rate was much faster (Table 4). Thus, Cr^{3+} was able to dominate rapidly the functional positions of the copolymer hydrogel, preventing diffusion of the other heavy metal ions into the copolymer hydrogel. Furthermore, its higher ionic charge and smaller atomic weight meant stronger electrostatic interaction (Chen et al. 2010). Thus, Cr^{3+} and Fe^{3+} were always more competitive than the other anions.

Adsorption mechanism

The change in FTIR peak from 1,043 to 1,039 cm^{-1} (Fig. 14) indicated that the $–SO_3H$ group from AMPS played an important role in the adsorption process. The phenomena on the asymmetric vibration absorption of carboxylate group shifting to lower wave number, as well as the symmetric vibration absorption of the carboxylate group that remained almost the same, represented the existence of the chelating interaction of carboxylate to heavy metal ions.

The formation of carboxylate coordination bonds with heavy metal ions reduced the charge density on the carboxylate oxygen, and then decreased its force constant (Huang et al. 2007). In addition, the weakened absorption bands of the reactive functional groups of the copolymer hydrogel disappeared after the adsorption process. This result indicated that these residual reactive functional groups were also involved in the adsorption process (Zheng et al. 2011). The mechanism of adsorption by the hydrogel involved ion exchange and chelation with heavy metal ions as predicted. Thus, the adsorption process of HEA/AMPS copolymer hydrogel was mainly due to the chemisorptions; however, physisorption was also involved in the process.

Conclusions

In this research, the experimental group A-2-d [70 % water volume ratio and (*n* (AMPS)/*n* (HEA)=1:1)] was the optimal adsorbent. When considering all kinds of metal ions, the optimal pH and temperature were 6.0 and 15 °C, respectively. Pb^{2+}, Cd^{2+}, Cu^{2+}, and Fe^{3}+ reached adsorption equilibriums within 24 h, whereas the comparative time for Cr^{3+} was 5 h. The maximum load capacity for Pb^{2}+, Cd^{2+}, Cr^{3+}, and Fe^{3+} was 1,000 mg L^{-1}, whereas that for Cu^{2+} was 500 mg L^{-1}. The priority order in multicomponent adsorption was Cr^{3+}>Fe^{3+}>Cu^{2+}>Cd^{2+}>Pb^{2+}. The adsorption process of HEA/AMPS copolymer hydrogel for heavy metal ions was mainly due to the chemisorption and partly due to physisorption. It also fitted the pseudo-second-order equation and the Langmuir adsorption isotherm very well.

Finally, the HEA/AMPS copolymer hydrogel in this research was concluded to be an effective adsorbent of heavy metal ions. The prepared novel HEA/AMPS copolymer hydrogel might have great potential applications in environmental work as smart adsorbent materials. The technique would be very useful in real life because heavy metal ion wastewater could be decontaminated effectively due to the HEA/AMPS copolymer hydrogel, which has high adsorption capacity and fast adsorption rate for various heavy metal ions. Furthermore, the radiation-induced copolymerization used in this research for the synthesis of HEA/AMPS copolymer hydrogel was a novel method and might provide

insight for further research in other fields of environmental science.

Acknowledgments This study was financially supported by Research projects of Department of Environmental Protection of Jiangsu Province (no. 201108) and Natural Science Foundation of Jiangsu Province (no. BK2010056).

References

Abdel-Halim ES, Al-Deyab SS (2011) Hydrogel from crosslinked polyacrylamide/guar gum graft copolymer for sorption of hexavalent chromium ion. Carbohyd Polym 86:1306–1312

Abdel-Halim ES, El-Rafie MH, Al-Deyab SS (2011) Polyacrylamide/guar gum graft copolymer for preparation of silver nanoparticles. Carbohyd Polym 85:692–697

Aguado J, Arsuaga JM, Arencibia A, Lindo M, Gascon V (2009) Aqueous heavy metals removal by adsorption on amine-functionalized mesoporous silica. J Hazard Mater 163:213–221

Ali I (2010) The quest for active carbon adsorbent substitutes: inexpensive adsorbents for toxic metal ions removal from wastewater. Sepn Purfn Rev 39:95–171

Ali I, Gupta VK (2006) Advances in water treatment by adsorption technology. Nat Protoco 1:2661–2667

Bozkurt A, Ekinci O, Meyer WH (2003) Synthesis and characterization of proton-conducting copolymers on the basis of vinylpyrrolidone and acrylamido sulfonic acid. J Appl Polym Sci 90:3347–3353

Cao J, Tan Y, Che Y, Xin H (2010) Novel complex gel beads composed of hydrolyzed polyacrylamide and chitosan: an effective adsorbent for the removal of heavy metal from aqueous solution. Bioresour Technol 101:2558–2561

Chen H, Xu ZY, Wan HQ, Zheng JZ, Yin DQ, Zheng SR (2010) Aqueous bromate reduction by catalytic hydrogenation over Pd/Al_2O_3 catalysts. Appl Catal B-Environ 96:307–313

El-Hag Ali A, Shawky HA, Abd El Rehim HA, Hegazy EA (2003) Synthesis and characterization of PVP/AAc copolymer hydrogel and its applications in the removal of heavy metals from aqueous solution. Eur Polym J 39:2337–2344

Essawy HA, Ibrahim HS (2004) Synthesis and characterization of poly (vinylpyrrolidone-co-methylacrylate) hydrogel for removal and recovery of heavy metal ions from wastewater. React Funct Polym 61:421–432

Freudlich H (1907) Ueber die adsorption in Loesungen. J Phys Chem C 7:385–470

Gupta VK, Ali I (2000) Utilisation of bagasse fly ash (a sugar industry waste) for the removal of copper and zinc from wastewater. Sepn Purifn Technol 18:131–140

Gupta VK, Ali I (2004) Removal of lead and chromium from wastewater using bagasse fly ash—a sugar industry waste. J Colloid Interf Sci 271:321–328

Gupta VK, Rastogi A (2008a) A Sorption and desorption studies of chromium (VI) from nonviable cyano bacterium *Nostoc muscorum* biomass. J Hazard Mater 154:347–354

Gupta VK, Rastogi A (2008b) Equilibrium and kinetic modelling of cadmium(II) biosorption by nonliving algal biomass *Oedogonium* sp. from aqueous phase. J Hazard Mater 153:759–766

Gupta VK, Rastogi A (2009) Biosorption of hexavalent chromium by raw and acid-treated green alga *Oedogonium hatei* from aqueous solutions. J Hazard Mater 163:396–402

Gupta VK, Suhas (2009) Application of low cost adsorbents for dye removal—a review. J Environ Manage 90:2313–2342

Gupta VK, Mohan D, Sharma S, Park KT (1999) Removal of chromium(VI) from electroplating industry wastewater using bagasse fly ash—a sugar industry waste material. Environmentalist 19:129–136

Gupta VK, Gupta M, Sharma S (2001) Process development for the removal of lead and chromium from aqueous solutions using red mud—an aluminum industry waste. Water Res 35:1125–1134

Gupta VK, Jain CK, Ali I, Sharma M, Saini VK (2003) Removal of cadmium and nickel from wastewater using bagasse fly ash—a sugar industry waste. Water Res 37:4038–4044

Gupta VK, Mittal A, Gajbe V, Mittal J (2006a) Removal and recovery of the hazardous azo dye acid orange 7 through adsorption over waste materials: bottom ash and de-oiled soya. Ind Eng Chem Res 45:1446–1453

Gupta VK, Mittal A, Kurup L, Mittal J (2006b) Adsorption of a hazardous dye, erythrosine, over hen feathers. J Colloid Interf Sci 304:52–57

Gupta VK, Ali I, Saini VK (2007a) Adsorption studies on the removal of Vertigo Blue 49 and Orange DNA13 from aqueous solutions using carbon slurry developed from a waste material. J Colloid Interf Sci 315:87–93

Gupta VK, Jain R, Mittal A, Mathur M, Sikarwar S (2007b) Photochemical degradation of the hazardous dye Safranin-Tusing TiO_2 catalyst. J Colloid Interf Sci 309:464–469

Gupta VK, Jain R, Varshney S (2007c) Electrochemical removal of the hazardous dye Reactofix Red 3 BFN from industrial effluents. Colloid Interf Sci 312:292–296

Gupta VK, Carrott PJM, Ribeiro Carrott MML (2009) Low cost adsorbents: growing approach to wastewater treatment—a review. Crit Rev Env Sci Tec 39:783–842

Gupta VK, Rastogi A, Nayak A (2010) Adsorption studies on the removal of hexavalent chromium from aqueous solution using a low cost fertilizer industry waste material. J Colloid Interf Sci 342:135–141

Gupta VK, Saleh TA, Ali I, Nayak A, Agarwal S (2012) Chemical treatment technologies for waste-water recycling—an overview. RSC Adv. doi:10.1039/C2RA20340E

Huang F, Zheng Y, Yang Y (2007) Study on macromolecular metal complexes: synthesis, characterization, and fluorescence properties of stoichiometric complexes for rare earth coordinated with poly (acrylic acid). J Appl Polym Sci 103:351–357

Ijagbemi CO, Baek MH, Kim DS (2010) Adsorptive performance of un-calcined sodium exchanged and acid modified montmorillonite for Ni^{2+} removal: equilibrium, kinetics, thermodynamics and regeneration studies. J Hazard Mater 174:746–755

Ju XJ, Zhang SB, Zhou MY, Xie R, Yang L, Chu LY (2009) Novel heavy metal adsorption material: ion-recognition P(NIPAM-co-BCAm) hydrogels for removal of lead(II) ions. J Hazard Mater 167:114–118

Kasgoz H, Ozgumus S, Orbay M (2003) Modified polyacrylamide hydrogels and their application in removal of heavy metal ions. Polymer 44:1785–1793

Kok Yetimoglu E, Kahraman MV, Ercan O, Akdemir ZS, Kayaman Apohan N (2007) N-vinylpyrrolidone/acrylic acid/2-acrylamido-2-methylpropane sulfonic acid based hydrogels: synthesis, characterization and their application in the removal of heavy metals. React Funct Polym 67:451–460

Langmuir I (1918) The adsorption of gases on plane surfaces of glass, mica and platinum. J Am Chem Soc 40:1361–1403

Miretzky P, Saralegui A, Cirelli AF (2006) Simultaneous heavy metal removal mechanism by dead macrophytes. Chemosphere 62:247–254

Mohan S, Sreelakshmi G (2008) Fixed bed column study for heavy metal removal using phosphate treated rice husk. J Hazard Mater 153:75–82

Ngah WS, Kamari A, Koay YJ (2004) Equilibrium and kinetics studies of adsorption of copper (II) on chitosan and chitosan/PVA beads. Int J Biol Macromol 34:155–161

Osifo PO, Webster A, van der Merwe H, Neomagus HW, van der Gun MA, Grant DM (2008) The influence of the degree of cross-linking on the adsorption properties of chitosan beads. Bioresour Technol 99:7377–7382

Pourjavadi A, Barzegar S (2009) Synthesis and evaluation of pH and thermosensitive pectin-based superabsorbent hydrogel for oral drug delivery systems. Starch 61:161–172

Rivas BL, Castro A (2003) Preparation and adsorption properties of resins containing amine, sulfonic acid, and carboxylic acid moieties. J Appl Polym Sci 90:700–705

Rueda CJ, Komber H, Cedron JC, Voit B, Shevtsova G (2003) Synthesis of new hydrogels by copolymerization of poly (2-methyl-2-oxazoline) bis (macromonomers) and *N*-vinylpyrrolidone. Macromol Chem Phys 204:947–953

Saleh TA, Gupta VK (2012) Column with CNT/magnesium oxide composite for lead (II) removal from water. Environ Sci Pollut Res 19:1224–1228

Srivastava SK, Gupta VK, Mohan D (1997) Removal of lead and chromium by activated slag—a blast-furnace waste. J Environ Eng 123:461–468

Wang Q, Xie X, Zhang X, Zhang J, Wang A (2010) Preparation and swelling properties of pH-sensitive composite hydrogel beads based on chitosan-*g*-poly (acrylic acid)/vermiculite and sodium alginate for diclofenac controlled release. Int J Biol Macromol 46:356–362

Yildi U, Kemika OF, Hazerb B (2010) The removal of heavy metal ions from aqueous solutions by novel pH-sensitive hydrogels. J Hazard Mater 183:521–532

Zhao Y, Su H, Fang L, Tan T (2005) Superabsorbent hydrogels from poly (aspartic acid) with salt-, temperature- and pH-responsiveness properties. Polymer 46:5368–5376

Zheng Y, Wang A (2010) Removal of heavy metals using polyvinyl alcohol semi-IPN poly (acrylic acid)/tourmaline composite optimized with response surface methodology. Chem Eng J 162:186–193

Zheng YA, Huang DJ, Wang AQ (2011) Chitosan-*g*-poly(acrylic acid) hydrogel with crosslinked polymeric networks for Ni^{2+} recovery. Anal Chim Acta 687:193–200